

## Survey of Uniformity of Pressure Profile in Wind Tunnel by Using Hot Wire Annometer Systems

Rao Yerrapragada. K.S.S<sup>1\*</sup>, S.N.Ch.Dattu .V<sup>2\*</sup>, Dr. B.Balakrishna<sup>3\*</sup>

<sup>1\*</sup>Aditya Engineering College, Associate Professor in Department of Mechanical Engineering, Andhra Pradesh.

<sup>2\*</sup>Pragati Engineering College, Associate Professor in Department of Mechanical Engineering, Andhra Pradesh.

<sup>3\*</sup>JNTU KAKINADA, Professor in Department of Mechanical Engineering, Andhra Pradesh

### ABSTRACT

The purpose of this research work is to investigate experimentally and computationally the uniformity of velocity profile in wind tunnel. A wind tunnel is an instrument used to examine the stream lines and forces that are induced as the fluid flows past a fully submerged body. The uni-insta's wind tunnel (300 mm\*300 mm) has been designed to give a large working section for the purpose of being able to layout substantial site models. The tunnel has a built in boundary layer simulation system that allows good simulation of the atmospheric velocity gradients. The tunnel is built around a sectionalized wooden frame work incorporating exterior grade plywood panels in the settling length and working section, clad in laminate on the side elevation for ease of maintenance. A bell mount entry incorporated is followed by a smooth settling length chamber comprising of well graded honey comb network fine mesh. The side panels of the working section are transparent acrylic cover, to gives a large viewing area .Additional matt back side panels gives photographic construct to smoke trails. The top panel of the working section is removable in order to fix the models.

**Keywords:** - uni-insta's wind tunnel, acrylic cover, stream lines.

### I. BACKGROUND

In 1941 the US constructed one of the largest wind tunnels at that time at Wright Field in Dayton, Ohio. This wind tunnel starts at 45 feet (14 m) and narrows to 20 feet (6.1 m) in diameter. Two 40-foot (12 m) fans were driven by a 40,000 H.P electric motor. Large scale aircraft models could be tested at air speeds of 400 mph (640 km/h).[5] The wind tunnel used by German scientists at Peenemünde prior to and during WWII is an interesting example of the difficulties associated with extending the useful range of large wind tunnels. It used some large natural caves which were increased in size by excavation and then sealed to store large volumes of air which could then be routed through the wind tunnels. This innovative approach allowed lab research in high-speed regimes and greatly accelerated the rate of advance of Germany's aeronautical engineering efforts. By the end of the war, Germany had at least three different supersonic wind tunnels, with one capable of Mach 4.4 (heated) airflows. [4]

By the end of World War Two, the US had built eight new wind tunnels, including the largest one in the world at Moffett Field near Sunnyvale, California, which was designed to test full size aircraft at speeds of less than 250 mph[7] and a vertical wind tunnel at Wright Field, Ohio, where the wind stream is upwards for the testing of models in spin situations and the concepts and engineering

designs for the first primitive helicopters flown in the US.[5] Later research into airflows near or above the speed of sound used a related approach. Metal pressure chambers were used to store high-pressure air which was then accelerated through a nozzle designed to provide supersonic flow. The observation or instrumentation chamber ("test section") was then placed at the proper location in the throat or nozzle for the desired airspeed. For limited applications, Computational fluid dynamics (CFD) can increase or possibly replace the use of wind tunnels. For example, the experimental rocket plane Space Ship One was designed without any use of wind tunnels. However, on one test, flight threads were attached to the surface of the wings, performing a wind tunnel type of test during an actual flight in order to refine the computational model. Where external turbulent flow is present, CFD is not practical due to limitations in present day computing resources. For example, an area that is still much too complex for the use of CFD is determining the effects of flow on and around structures, bridges, terrain, etc. The most effective way to simulative external turbulent flow is through the use of a boundary layer wind tunnel. There are many applications for boundary layer wind tunnel modeling. For example, understanding the impact of wind on high-rise buildings, factories, bridges, etc. can help building designers construct a structure that stands up to wind effects in the most efficient manner possible. Another significant

application for boundary layer wind tunnel modeling is for understanding exhaust gas dispersion patterns for hospitals, laboratories, and other emitting sources. Other examples of boundary layer wind tunnel applications are assessments of pedestrian comfort and snow drifting. Wind tunnel modeling is accepted as a method for aiding in Green building design. For instance, the use of boundary layer wind tunnel modeling can be used as a credit for Leadership in Energy and Environmental Design (LEED) certification through the U.S. Green Building Council. Wind tunnel tests in a boundary layer wind tunnel allow for the natural drag of the Earth's surface to be simulated. For accuracy, it is important to simulate the mean wind speed profile and turbulence effects within the atmospheric boundary layer.

Most codes and standards recognize that wind tunnel testing can produce reliable information for designers, especially when their projects are in complex terrain or on exposed sites. In the USA many wind tunnels have been decommissioned in the last 20 years, including some historic facilities. Pressure is brought to bear on remaining wind tunnels due to declining or erratic usage, high electricity costs, and in some cases the high value of the real estate upon which the facility sits. On the other hand CFD validation still requires wind-tunnel data, and this is likely to be the case for the foreseeable future. Studies have been done and others are under way to assess future military and commercial wind tunnel needs, but the outcome remains uncertain.[6] More recently an increasing use of jet-powered, instrumented unmanned vehicles ["research drones"] has replaced some of the traditional uses of wind tunnels.[7]

## II. OPERATION OF WIND TUNNEL

Mount the model as per requirements. Calibrate the strain gauge balance to indicate an initial value of life force = 25kg, drag force = 2kg. Connect the pressure tapings to the manometer board and note the angle of incidence or angle of attack and set the smoke generator for operation. Then start the axial flow fan by switching on the starter switch. Note down the differential manometer readings, to calculate the free stream velocity  $V=C\sqrt{2gh}$ . Adjust the side window opening by operating the handle connected to it. Note the readings of the simple u-tube manometer which is connected to the pressure tapings. Repeat the procedure by adjusting the velocity and also for different angles of incidence.

## III. LITERAL SURVEY

According to E.G.Tulapurkara, assistant professor in IIT (Madras) experimental investigation of morels method for wind tunnel contraction the

following thesis were made for improve the design of a good wind tunnel. The contraction on the nozzle is an important component of a wind tunnel. As the flow passes through the contraction it accelerates and this results in a reduction of non-uniformity and turbulence level of the stream. In practical contractions, which are of finite length, one finds that adverse pressure gradients are present at the ends of the contraction (Bradshaw and Pankhurst, 1964). The axial velocity is higher than the velocity near the wall at the entry to the contraction and at the exit the velocity near the wall (i.e.; outside the boundary layer) is higher than that on the axis.

Thus for a good performance nozzle contour should give low adverse pressure gradients at the ends of contraction so that no separation of flow takes place, the boundary layer thickness at the exit should be small and non-uniformity in the velocity distribution at the exit must be small.. A good contour should achieve these with a small length to upstream diameter (D1) ratio nearly fifteen methods to obtain the shape of contraction. Bradshaw and Pankhurst (1964) recommended a contraction ratio of 12 for a good low turbulence wind tunnel. However, many wind tunnels in common use have smaller contraction ratios of the order of 4. Hence contractions with area ratio of 12 and T2 i.e., 3.434 are chosen for the present investigation. The diameter of the settling chamber ahead of the contraction is 250mm. Velocity in settling chamber is 4m/sec. Hence the value of Cpl. Based on experience of Tulapurkara (1980) and the recommendation of morel (1975) an acceptable value for the exit no uniformity is chosen as 2%. This requires the CPC to be less than 0.057. A value of 0.005 for Cpc is chosen. These values of CPL and CPC give the  $X=0.537$  and  $L/D1=0.858$  for  $C=12$  and  $X=0.332$  and  $L/D1=0.858$ . We get D2 equal to 72.17mm and 134.32m similarly experimental setup and technique. The velocity in settling chamber is 4m/s. This would be nearly the settling chamber velocity is most of wind tunnels with test section speed between 50 to 60 m/s and contraction ratio between 12 to 16. The velocity distribution at ends of contraction ratio and along the axis is obtained from measurements of total pressure and static pressure using PILIOL and static tubes. Micrometer FC012 made by Furness control LTD of UK are used for pressure tubes. Typical readings of manometer during velocity measurement near the inlet and exit were 1.3 0.5. The velocity distribution at the ends and distribution of axial velocity and wall velocity along the contraction are shown and  $C=3.464$  respectively R1 and R2 in these figures are the radii of contraction at inlet and exit.

#### IV. HOTWIRE ANENOMETER SYSTEM

The turbulence measurement in the boundary layer and in the wake region was carried out using the hot wire anemometer. The hot wire anemometer system consists of the following modules. 56C01 Constant Temperature Anemometer (Two No's) , 56C17 Bridge (Two No's), 56N21 linearizer (Two No's) , 56N20 signal conditioner (Two No's) , 56N23, Analog Processer Unit, 56N22 Mean Value Unit , 56N25 RMS Unit.

#### V. PRESSURE MEASUREMENT

The transverse mechanism was ended upon the test section of the tunnel. The probe was tightened to the transverse mechanism and introduced vertically into the Test section of the wind tunnel. Five hose connections were made between probe and the manometer. All leakages in the wind tunnel were checked and sealed. The start button was pushed on and the following parameters were entered into record by transferring the probe from 5mm at the top of the test section of wind tunnel to 300 mm bottom of test section in 6 steps.

TABULAR COLUMN:

Distance of Probe Traversed ( Y) mm	Pressure P1 In Mega bars (mbar)	Pressure P2 In Mega bars (mbar)	Pressure P3 In Mega bars (mbar)	Pressure P4 In Mega bars (mbar)	Pressure P5 In Mega bars (mbar)	Total Pressure (PT) In Mega bars ( mbar)	Static Pressure (Ps) In Mega bars (mbar)
5	-32.5	-45.6	-45.6	-34.2	-33	-32.45	-32.39
61	-32.4	-46.5	-46.5	-34.3	-32.7	-32.39	-32.35
122	-33	-46.3	-46.3	-34.3	-32.6	-32.9	-32.9
183	-32.3	-46.6	-46.6	-34	-32.8	-32.89	-32.8
244	-31.9	-44.3	-44.3	-33.8	-32.3	-31.89	-31.84
300	-42.6	-44.1	-44.1	-43.6	-43.4	-42.6	-42.53

Table No: 1

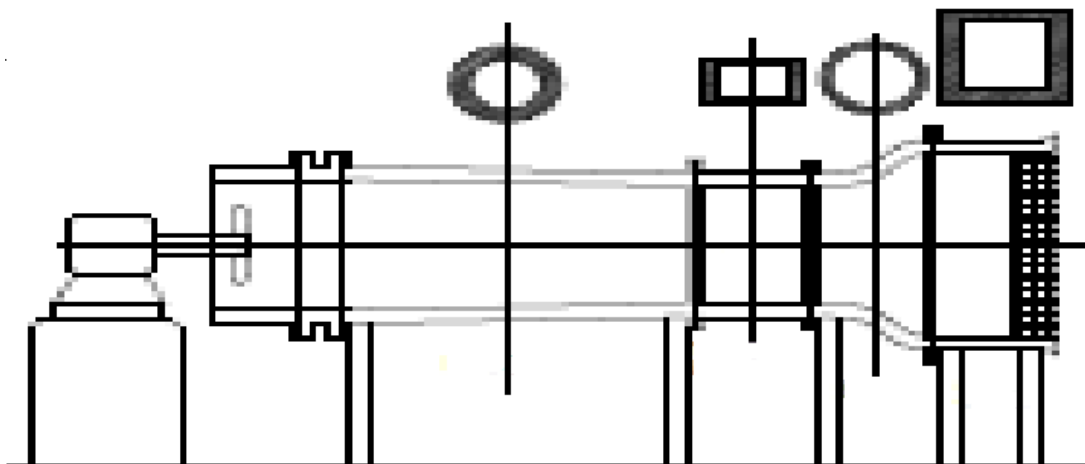


Figure No: 1 LINE SKETCH OF A WIND TUNNEL

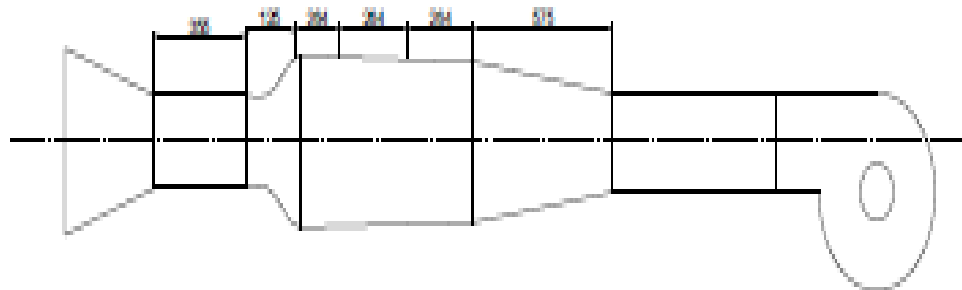


Figure No: 2 EXPERIMENTAL SET UP

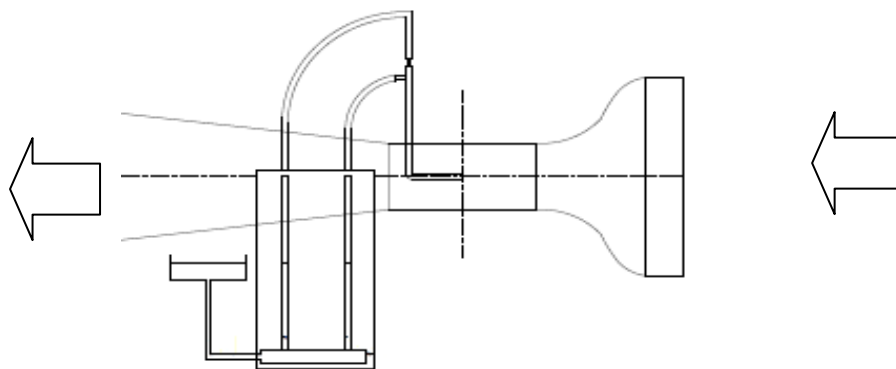


Figure No : 3 TEST FOR FINDING THE TUNNEL SPEED

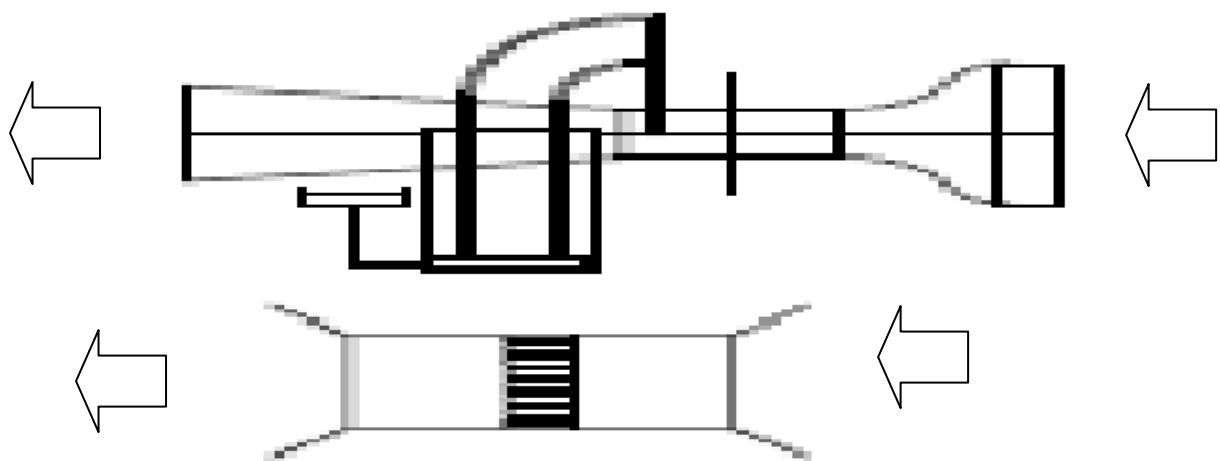
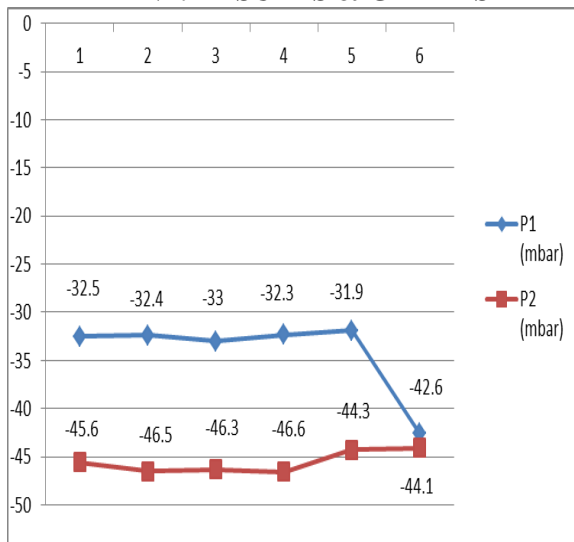
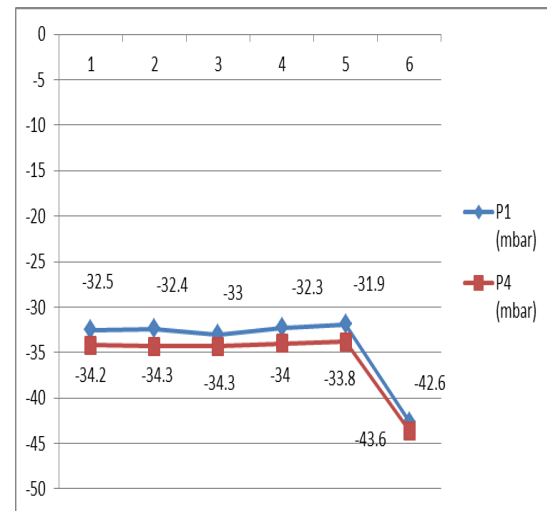


Figure No 4: VELOCITY DISTRIBUTION CURVE

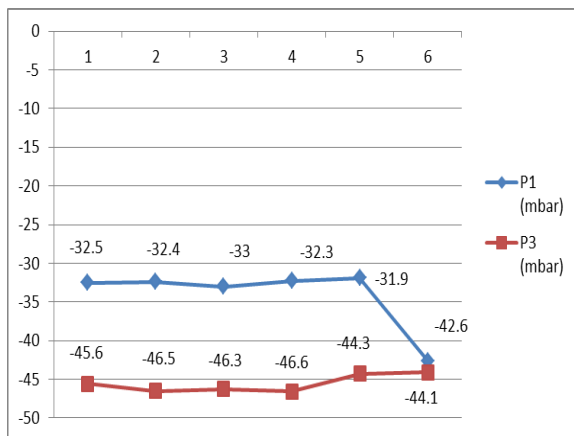
**VI. RESULTS & GRAPHS**



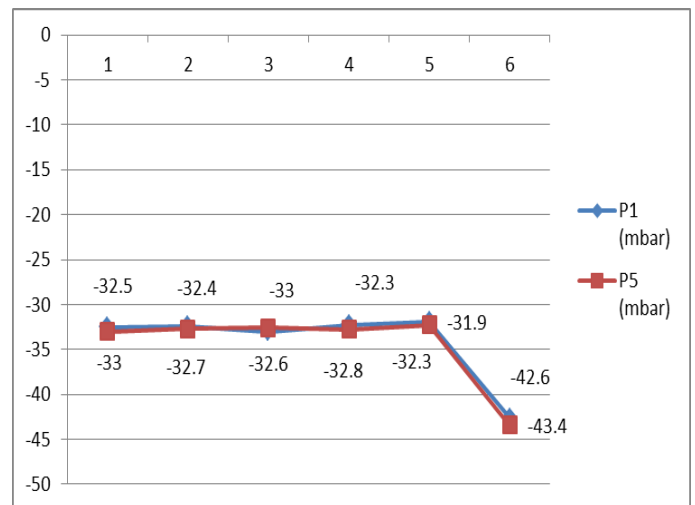
Graph 1 : Average P1 = -34.12 mbar  
 Average P2 = -45.57 mbar



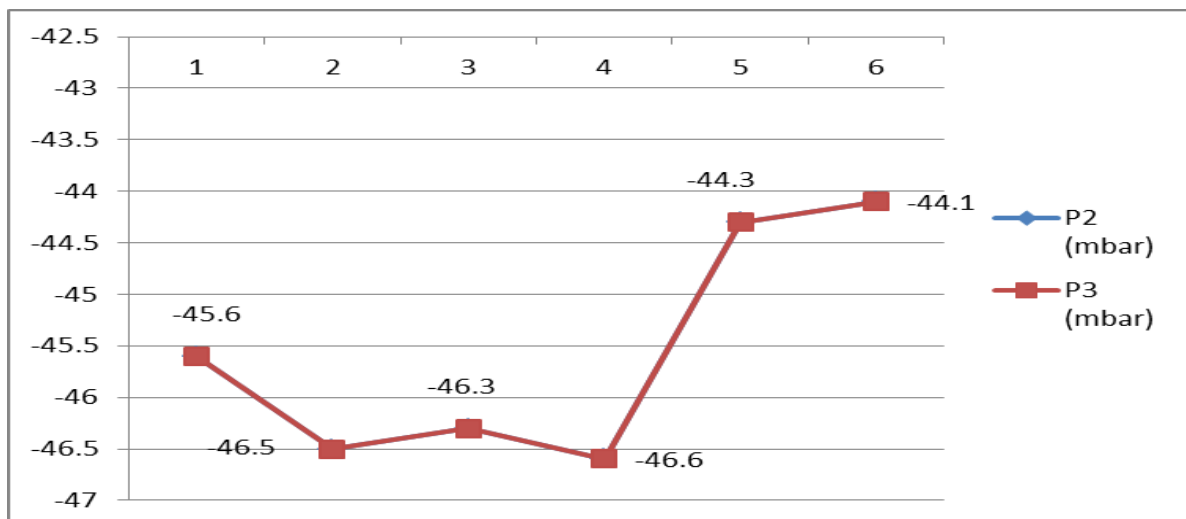
Graph3 : Average P1 = -34.12 m bar  
 Average P4 = -35.7 m bar



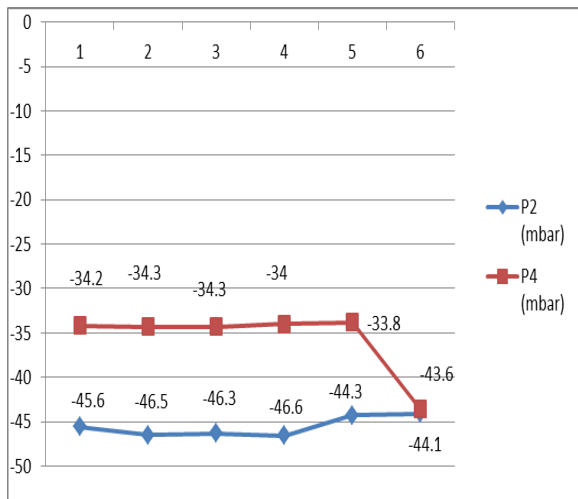
Graph2 : Average P1 = -34.12 m bar  
 Average P3 = -45.57 m bar



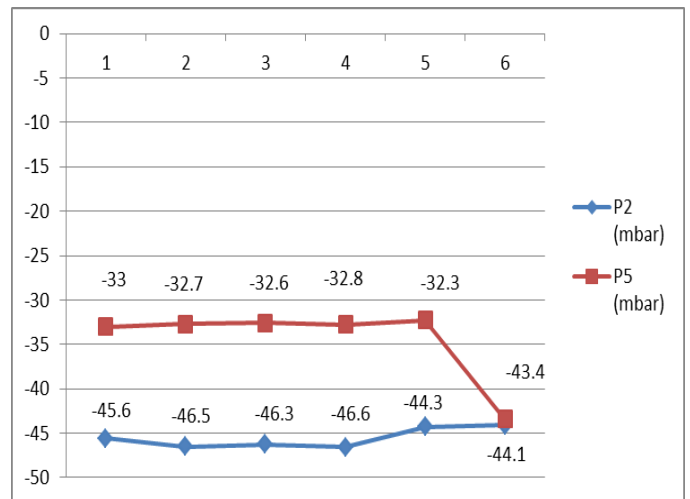
Graph4 : Average P1 = -34.12 m bar  
 Average P5 = -34.47 m bar



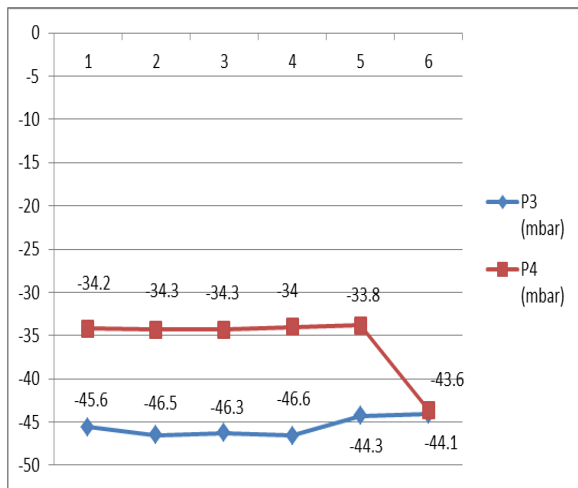
Graph5 : Average P2 = -45.57 m bar  
 Average P3 = -45.57 m bar



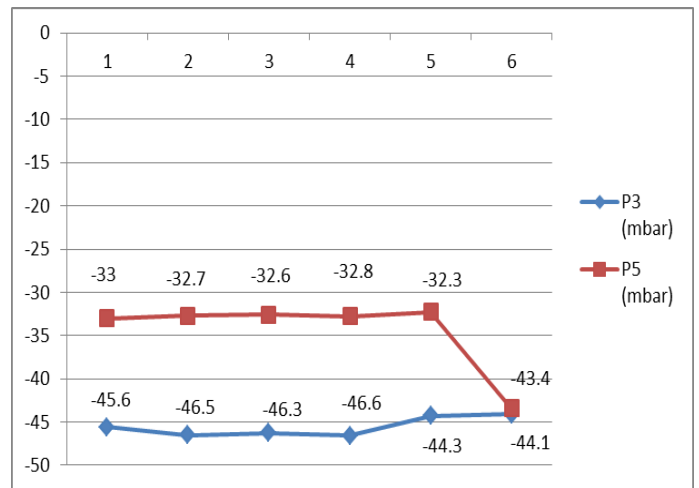
Graph6 : Average P2 = - 45.57 m bar  
 Average P4 = - 35.7 m bar



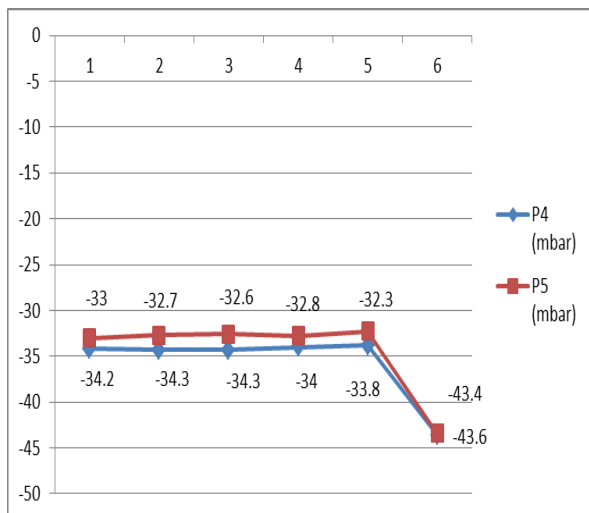
Graph7 : Average P2 = - 45.57 m bar  
 Average P5 = - 34.47 m bar



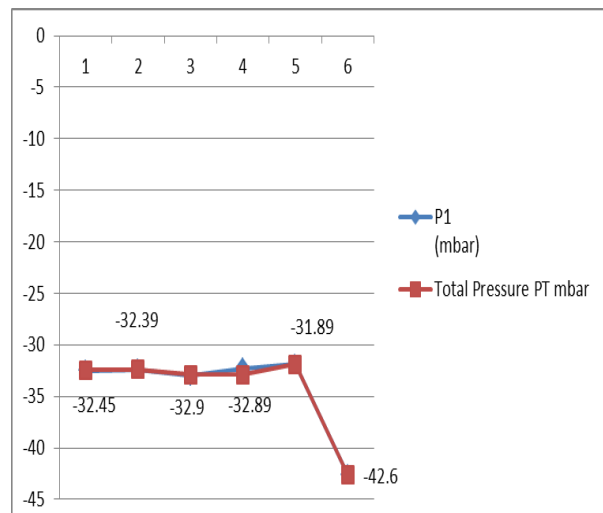
Graph8 : Average P3 = - 45.57 m bar  
 Average P4 = - 35.7 m bar



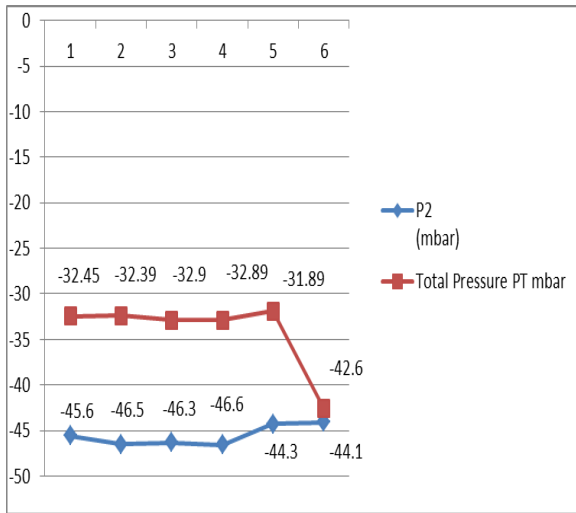
Graph9 : Average P3 = - 45.57 m bar  
 Average P5 = - 34.47 m bar



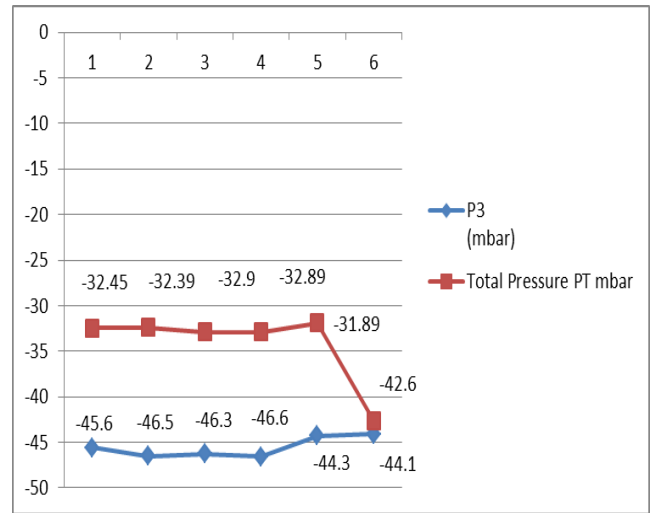
Graph10 : Average P4 = - 35.7 m bar  
 Average P5 = - 34.47 m bar



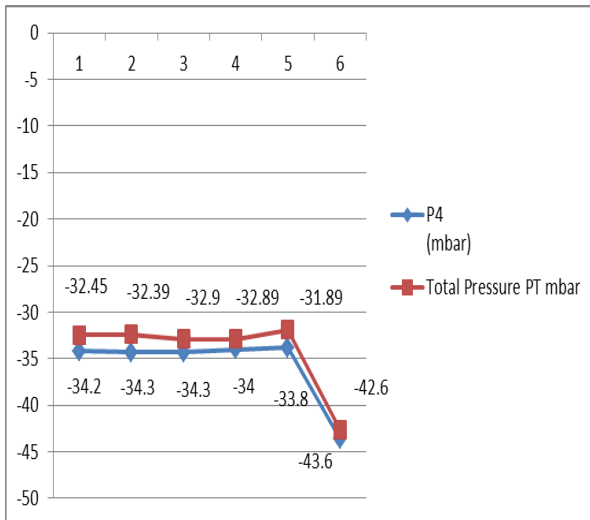
Graph11 : Average P1 = - 34.12 m bar  
 Avg Total Pressure( PT) = - 34.18 m bar



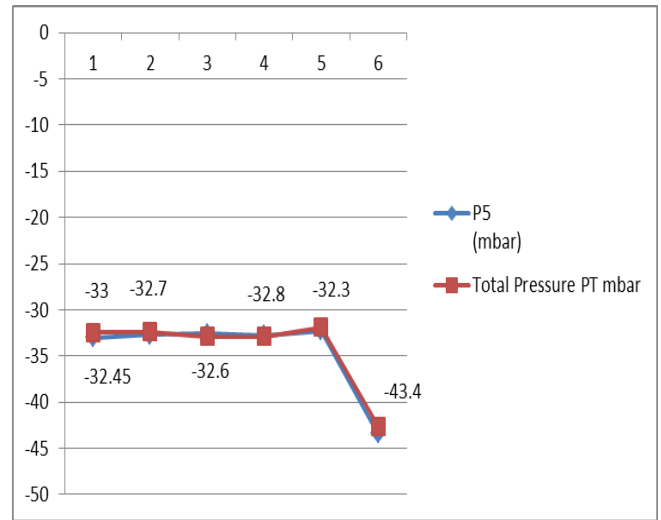
Graph12 : Average P2 = - 45.57 m bar  
 Avg Total Pressure ( PT ) = - 34.18 m bar



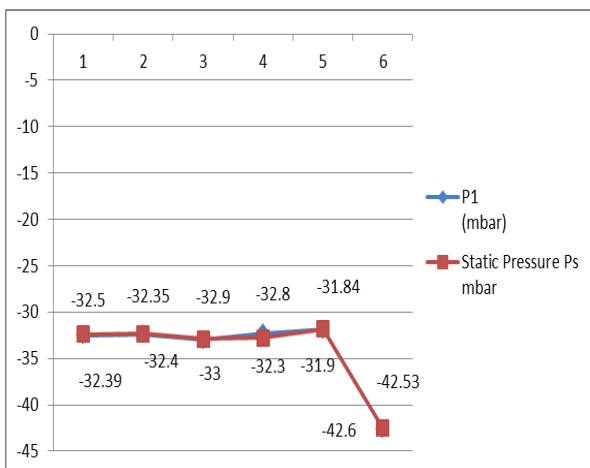
Graph13 : Average P3 = - 45.57 m bar  
 Avg Total Pressure ( PT ) = - 34.18 m bar



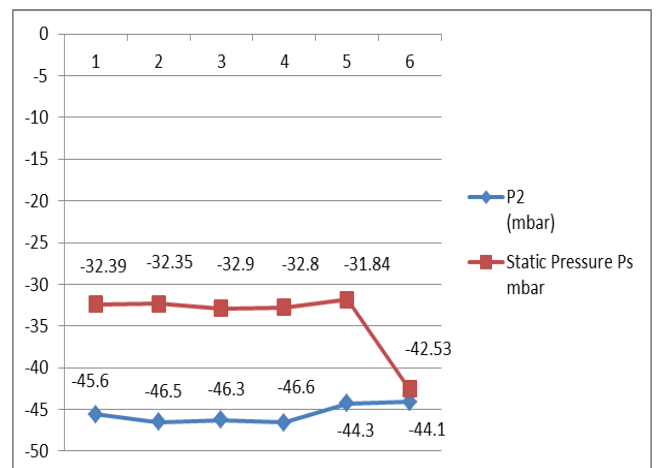
Graph14 : Average P4 = -35.7 m bar  
 Avg Total Pressure ( PT ) = - 34.18 m bar



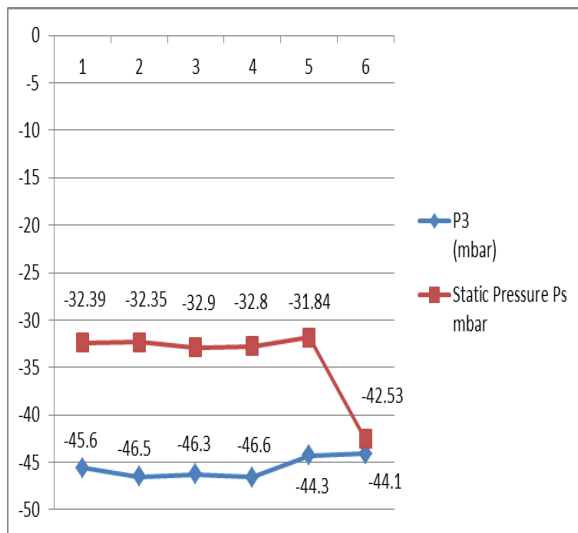
Graph15 : Average P5 = - 34.47 m bar  
 Avg Total Pressure ( PT ) = -34.18 m bar



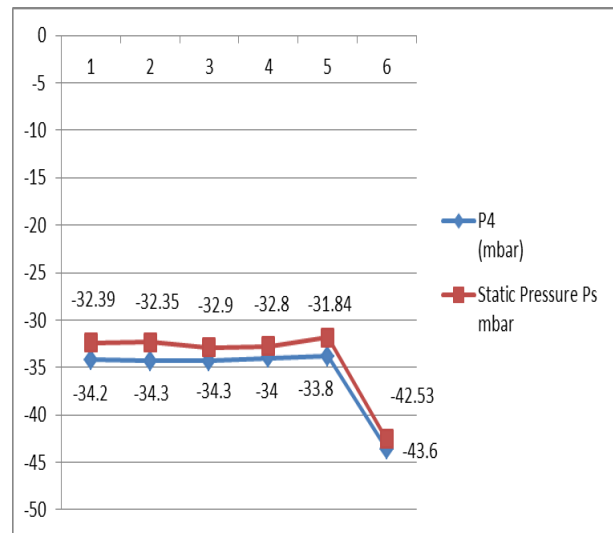
Graph16 : Average P1 = - 34.12 m bar  
 Avg Static Pressure ( PS ) = - 34.13 m bar



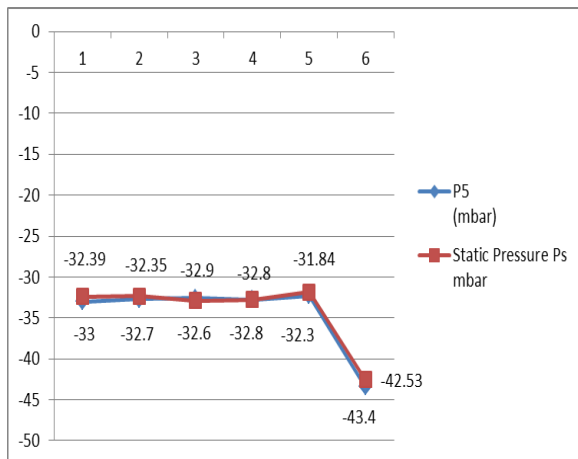
Graph17 : Average P2 = -45.57 m bar  
 Avg Static Pressure ( PS ) = - 34.13 m bar



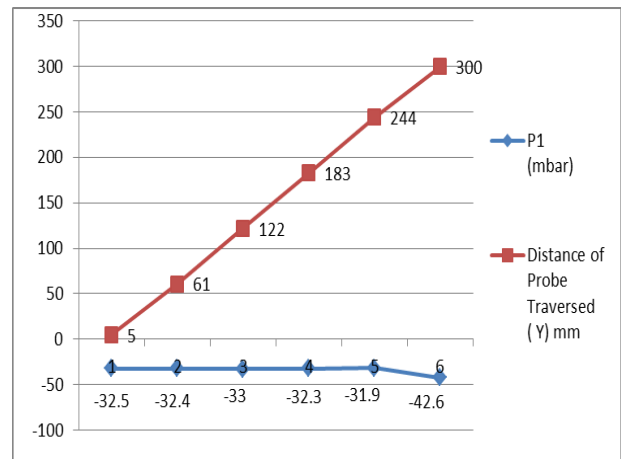
Graph18 : Average P3 = - 45.57 m bar  
 Avg Static Pressure ( PS ) = - 34.13 m bar



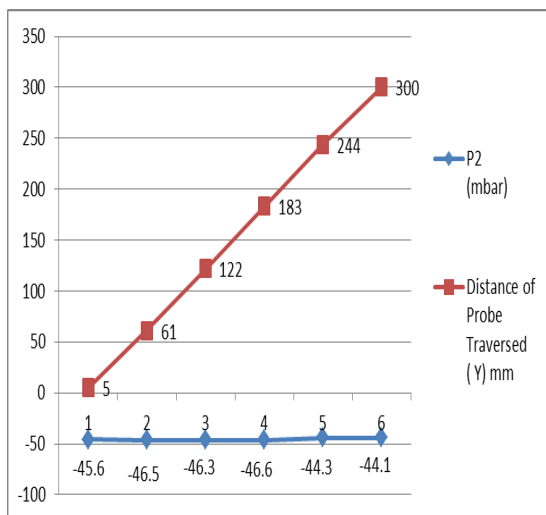
Graph19 : Average P4 = -35.7 m bar  
 Avg Static Pressure ( PS ) = -34.13 m bar



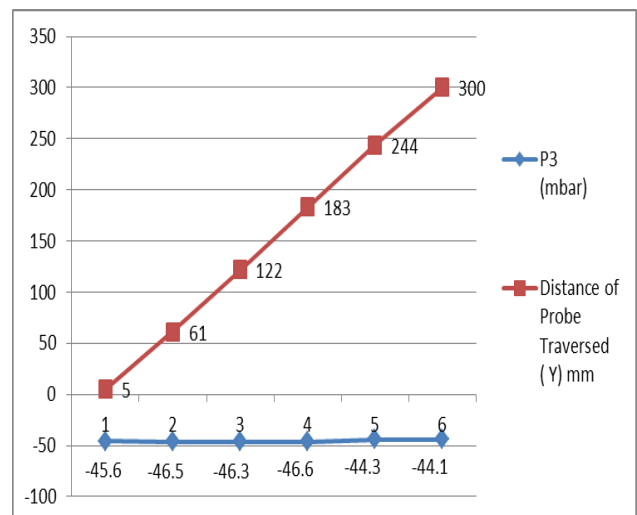
Graph20 : Average P5 = - 34.47 m bar  
 Avg Static Pressure ( PS ) = -34.13 m bar



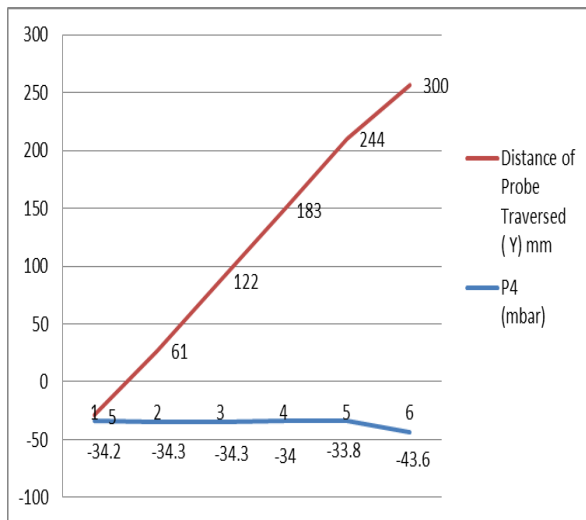
Graph21 : Average P1 = - 34.12 m bar  
 Avg Distance of Probe = 152.5 mm



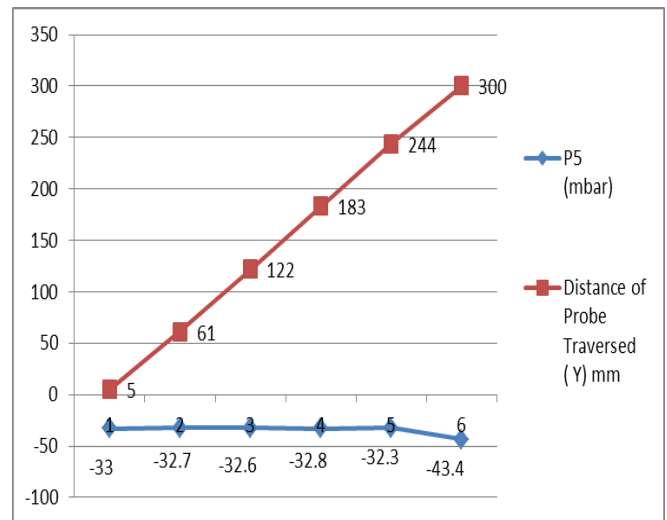
Graph22 : Average P2 = - 45.57 m bar  
 Avg Distance of Probe = 152.5 mm



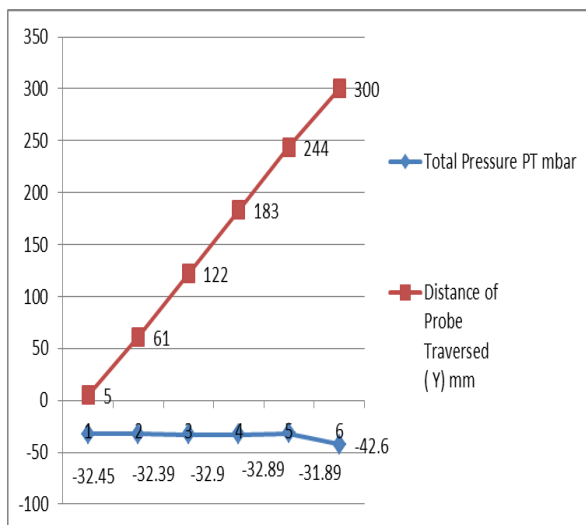
Graph23 : Average P3 = - 45.57 m bar  
 Avg Distance of Probe = 152.5 mm



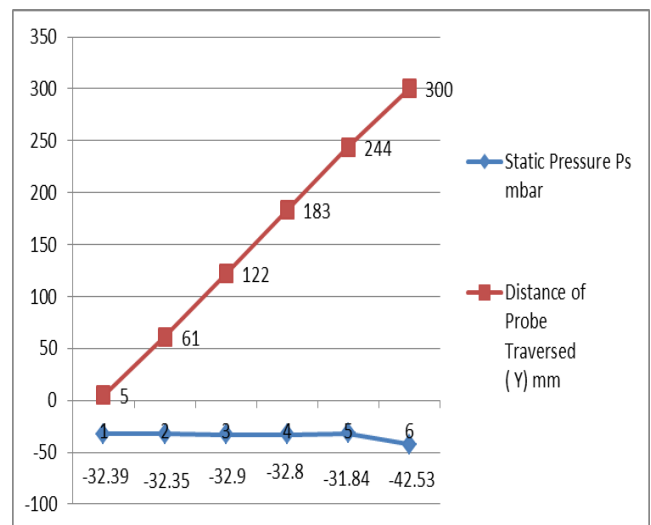
Graph24 : Average P4 = - 35.7 m bar  
 Avg Distance of Probe = 152.5 mm



Graph25 : Average P5 = - 34.47 m bar  
 Avg Distance of Probe = 152.5 mm



Graph26 : Average PT = - 34.18 m bar  
 Avg Distance of Probe = 152.5 mm



Graph27 : Average PS = - 34.13 m bar  
 Avg Distance of Probe = 152.5 mm

## VII. CONCLUSION

We find the average actual static pressure value is -34.13 m bar and average total pressure value is -34.18 mbar. The pressure variations at positions P2 & P3 are identical. Similarly at positions P1, P4, P5 found small marginal changes. We analyze that the pressure distribution of fluid is uniform. We can see clear picture of deviation in the graphs plotted as Pressure and its components Vs. the transverse distance of the probe in the test section of the wind tunnel.

## VIII. REASON FOR NONUNIFORMITY FLOW OF FLUID

The reason behind is may be due to the poor design of the wind tunnel section side. The contact ratio must be around 16 for to get a uniform flow.

But the contact ratio our wind tunnel is around 9. i.e.,  $a_1 = 900 \times 900$  mm,  $a_2 = 300 \times 300$  mm. The contact ratio =  $a_1/a_2 = 9$  which is below the required. It is also due to the poor design of the suction side.

## REFERENCES

- [1] Bossel. H.H. 1969 "Computations of Axisymmetric Contractions," AIAA Journal Volume 7 no.10 PP 2017-2020.
- [2] Bradshaw. P & Pankhurst.R.C. 1964, "The Design of Low Speed Wind Tunnels", Progress in Aeronautical Sciences Volume 5. Kuchenmann.D and Sterne. L.H.G Editors Pergamum Press PP 1-69.
- [3] Chmiclewski, GE 1974, "Boundary Layer Consideration in design of Aerodynamic

- Contractions”, Journal of Air Craft Volume 11 No 8 PP 435-438.
- [4] Kiein A. Ramjee. V & Venkataramani, K.S 1973, “Ann Experimental Study of Subsonic Flow in the axisymmetric contractions”, Flow volume 21 no 9 PP 312-320.
- [5] Morel T 1975 comprehensive Design of Axisymmetric Wind Tunnel Contractions”
- ASME JOURNAL OF FLUID ENGINEERING, Volume 97 No2 225-233.
- [6] Startford B.S 1959.The Prediction of Separation of Fluid Mechanics, Volume Part 1 PP 1-16
- [7] Thwaltes B 1946, on Design of Contraction for Wind Tunnels, Aeronautical Research council, London R SM 2278.